

A Combined Meshless RBF-FDTD Method for the Analysis of Transient Electromagnetic Fields

Khalef, R.^{1*}, Benkhawa, L.², Grine, F.², Benhabiles, M. T.² and Riabi, M. L.²

¹*Doctoral School of Technology and Space Applications, Faculty of Technology Sciences, Department of Electronic, Laboratory of Electromagnetism and Telecommunications, University of Constantine1, Algeria, Road Ain El Bay, 25000, Constantine, Algeria*

²*Faculty of Technology Sciences, Department of Electronic, Laboratory of Electromagnetism and Telecommunications, University of Constantine1, Algeria, Road Ain El Bay, 25000, Constantine, Algeria*

ABSTRACT

A Meshless Time Domain Method is used in the local support domain to solve Maxwell's equations for one-dimensional transient electromagnetic problems. The approach is based on a combination of the Meshless Radial Basis Functions and the Leapfrog time-stepping scheme for the Finite-Difference approximation of the first order partial derivatives. A comparison is performed between the conventional FDTD and RBF's with Gaussian, Wendland-C4 Compactly Supported RBF (CSRBF) and Inverse Multi-Quadric (IMQ) basis functions. The numerical results showed that the proposed method provides an accurate solution for transient electromagnetic problems.

Keywords: Finite-Difference-Time-Domain, Local Support, Meshless method, Compact support RBF, Inverse Multi-Quadric, Transient Electromagnetic Field

INTRODUCTION

During the last decade, several methods have been proposed to solve Maxwell equations in complex radiating structures, without the use of finite element meshes. Such Meshless approaches distinguish four main methods based on a Galerkin variational formulation:

- √ The Moving Least-Squares approximations, which regroup fundamentally the Diffuse Element Method DEM, and the Element Free Galerkin Method EFGM (Cingoski et al., 1998).

Article history:

Received: 17 February 2016

Accepted: 22 April 2016

E-mail addresses:

kh.rostom@gmail.com (Khalef, R.),

benkhaouadj@yahoo.fr (Benkhawa, L.),

faroukgrine@umc.edu.dz (Grine, F.),

mt.benhabiles@umc.edu.dz (Benhabiles, M. T.),

ml.riabi@yahoo.fr (Riabi, M. L.)

*Corresponding Author

- √ The Reproducing Kernel Method RKM, or Smooth Particle Hydrodynamics (Belytschko et al., 1996).
- √ Methods constructed from a purely polynomial interpolation, Point Interpolation Method PIM (Liu & Gu, 1999), (Lima et al., 2012).
- √ Mixed methods coupling radial basis functions, either with a moving least square approximation (Kansa, 1990; Kansa, 1992; Fasshauer, 2007; Liu & Gu, 2005), or with a polynomial interpolation (Viana et al., 2006; Wang & Liu, 2001; Wendland, 1995).

The purpose of this paper is to apply the explicit Meshless RBF (Radial Basis Function) method, with three types of local support of basis functions, namely Gaussian, Wendland – C4 CSRBF and IMQ, to solve time domain Maxwell equations in one dimension. The rationale for this project is to check the stability problems related with last basis functions in local support domain and to provide the best solutions for the analysis of transient electromagnetic problems. Additionally, the RBF method is very economical in terms of computation time and programming burden in comparison with the conventional Finite-Difference Time-Domain (FDTD) method. The present research also attempts to shed light on the errors of the FDTD method.

The present project is structured as follows. The first section provides a brief overview of the RBF method with a description of the shape function with its derivative; the local support domain will be presented in the same section. Section three is equated to the time domain equations for the electromagnetic field in one dimension and the criterion of stability condition of time. Section four discusses the use of 1-D electromagnetic case to estimate the accuracy and efficiency of the proposed method by comparing the results of the proposed method with that of the FDTD, and the RBF with global support basis function at (Lai et al., 2008) with regard to the PEC boundary conditions and time-exponential current excitation. The last section presents a general conclusion about the results of the present study.

THE MESHLESS METHOD BASED ON RBF

The RBF approximation function $\mathbf{u}^h(\mathbf{x})$ can be expressed as follows:

$$\mathbf{u}^h(\mathbf{x}) = \sum_{l=1}^N \varphi_l(\mathbf{x}) \cdot \mathbf{a}_l, \quad \forall \mathbf{x} \in \mathbf{R}^d \quad [1]$$

where $\varphi_l(\mathbf{x}) = \varphi(\|\mathbf{x} - \mathbf{x}_l\|)$ is the radial basis function centred at the collocation nodes $x_1, x_2, \dots, x_N \in \mathbf{R}^d$, \mathbf{a}_l are unknown coefficients to be computed and represents the Euclidean distance between test points x and node points x_l .

In order to determine the coefficients \mathbf{a}_l we force the interpolation to pass through all the N collocation points, resulting in

$$\mathbf{u}^h(\mathbf{x}) = \boldsymbol{\varphi}^T \mathbf{A}^{-1} \mathbf{u}_e = \mathbf{N}(\mathbf{x}) \mathbf{u}_e \quad [2]$$

where $\mathbf{u}_e = [\mathbf{u}(\mathbf{x}_1), \mathbf{u}(\mathbf{x}_2), \dots, \mathbf{u}(\mathbf{x}_N)]^T$,

$$A = \begin{bmatrix} \varphi_1(x_1) & \varphi_2(x_1) & \dots & \varphi_N(x_1) \\ \varphi_1(x_2) & \varphi_2(x_2) & \dots & \varphi_N(x_2) \\ \vdots & \vdots & \ddots & \vdots \\ \varphi_1(x_N) & \varphi_2(x_N) & \dots & \varphi_N(x_N) \end{bmatrix}_{N \times N} \quad [3]$$

and $N(x) = [N_1, \dots, N_j, \dots, N_N]$ is the matrix of shape function, that is to satisfy the delta function property. The vector u_e holds the field values at N node locations in the surrounding domain of influence around x .

Figure 1 represents the local support domain.

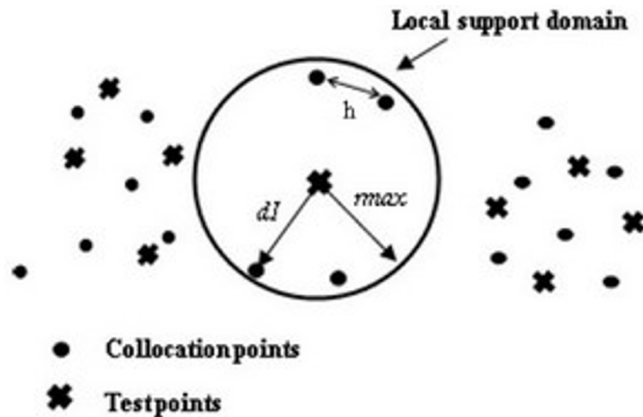


Figure 1. Schematic Illustration of the Local Support Domain with Radius r_{max} , Average Node Distance h and Distance d_l between Collocation Points and Test Points

In this work, the formula $u^h(x)$ can be any component of the electric and magnetic fields, the spatial derivatives of electric and magnetic fields needed to solve Maxwell’s equations. The partial derivative of $u^h(x)$ is only related to shape function matrix. Where, the first – order derivative of this function in x direction can be expressed as (Lai et al., 2008):

$$\frac{\partial u^h(x)}{\partial x} = \frac{\partial N(x)}{\partial x} \quad [4]$$

where

$$\frac{\partial N(x)}{\partial x} = \left[\frac{\partial \varphi_1(x)}{\partial x}, \frac{\partial \varphi_2(x)}{\partial x}, \dots, \frac{\partial \varphi_N(x)}{\partial x} \right] \quad [5]$$

THE TIME DOMAIN FIELD FORMULATION IN ONE DIMENSION

The one-dimensional transient electromagnetic problem in a homogenous isotropic medium is tackled as a TEM wave. According to Cartesian coordinates, the wave is polarised along the y direction, and it propagates along the x direction. Consequently, the problem is independent of the z variable, and Maxwell’s set reduces to only two equations where the time derivatives in RBF meshless method can be approximated by central differences in leapfrog time stepping

scheme similar to FDTD method. The resulting explicit discretisation formulation of those equations can be derived by the following equations (Kaufmann et al., 2012):

$$H_{z,i}^{n+\frac{1}{2}} = H_{z,i}^{n-\frac{1}{2}} - \frac{\Delta t}{\mu} \left[\sum_{j=1}^{n_{As}} \partial x N_{E,i}^j E_{y,j}^n \right] \tag{6}$$

$$E_{y,i}^{n+1} = E_{y,i}^n - \frac{\Delta t}{\epsilon} \left[\sum_{j=1}^{n_{As}} \partial x N_{H,i}^j H_{z,j}^{n+\frac{1}{2}} + J_y^{n+\frac{1}{2}} \right] \tag{7}$$

where i is the current node locations, n is the time step and j the index in local support domain in Figure 1. An acceptable time-step Δt for the stability of leapfrog scheme is derived from the Neumann condition as $\Delta t \leq d_{\min,i} \sqrt{\mu\epsilon}$, where $d_{\min,i}$ is the shortest distance between any two collocation points in the domain (Shaterian et al., 2012).

NUMERICAL EXAMPLE

In order to confirm the proposed method, comparison of simulation results was carried out between the Meshless RBF with three types of basis function (Gaussian, Wendland-C4 CSRBF, IMQ) and the FDTD on a 1-D perfect electric conductor. The tangential electric field component must be zero at the boundary collocation points with each time-step update (Lai et al., 2008):

In Figure 2, the distribution of collocation points and test points is uniform. We suppose that N_x is the number of collocation points and that n_x is the test points whereas, h is the distance between two successive collocation points.

The computation region is one-metre long, the current excitation point is at $J_p (x = 0.35m)$ and the measurement point is at $obs (x = 0.85m)$ (Lai et al., 2008).

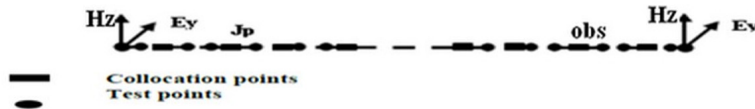


Figure 2. Distribution of collocation and test points in one dimension

The excitation source is a Gaussian pulse. Accordingly; we used three kinds of basis functions with a local support domain, namely Gaussian, Wendland-C4 CSRBF, and IMQ.

The Gaussian pulse of excitation is expressed by:

$$J_y(t) = \exp \left[-\left(\frac{t-t_0}{T} \right)^2 \right] \quad (\text{A/m}^2) \tag{8}$$

where: $t_0=3 \times 10^{-9}$ (s), $T=0.5 \times 10^{-9}$ (s)

In the present study, the following three types of radial basis functions (Gaussian, Wendland-C4 CSRBF and IMQ) are expressed by:

$$\varphi_l(x) = \exp(-s \cdot r_l^2) \tag{9}$$

$$\varphi_l(x) = \left[1 - \left(\frac{r_l}{\delta} \right) \right]^6 \left[3 + 18 \left(\frac{r_l}{\delta} \right) + 35 \left(\frac{r_l}{\delta} \right)^2 \right] \tag{10}$$

$$\varphi_I(x) = \frac{1}{\sqrt{1+(e.r_I)^2}} \quad [11]$$

where s, δ and e are the shape parameters of the above basis functions successively.

And $r_I = \frac{d_I}{r_{max}}$, where r_{max} represents the local support domain radius at collocations points $x_I, d_I = \|x_I - x\|$ is the distance between the test points and the collocations points.

Based on the analysis in this section, it can be inferred that the number of collocation points N_x represents the number of electric field E -points, and the number of test points n_x represents the number of magnetic field H -points. In the electromagnetic computation, the shape parameters s in the Gaussian function, δ in the Wendland-C4 function and e in the IMQ function, have to be adjusted carefully in order to achieve a sum of shape functions equal to unity and subsequently to ensure the stability of the computational scheme. In the following, we will choose their parameters to obtain the best results.

RESULTS AND DISCUSSION

The input data used for the computation of the plots presented in Figures 3-5 are $N_x=101, n_x=100, r_{max}=1.1h$. Figure 3 shows a comparison of the results for the E_y component in the observation point *obs1* for the effective odd oscillations 20 periods in PEC boundary condition between:

1. Three different types of local support basis functions, Gaussian, Wendland-C4 CSRBF, and IMQ, for which we obtained identical results.
2. For RBF method and the traditional FDTD method, we had obtained the same results.
3. The same as the previously obtained result from RBF-FDTD method with the data from (Lai et al., 2008), Figure 3-5-a and we found them similar, although the radial basis function from (Lai et al., 2008), is of global support, and the number of collocation and test points differs (Lai et al., 2008).

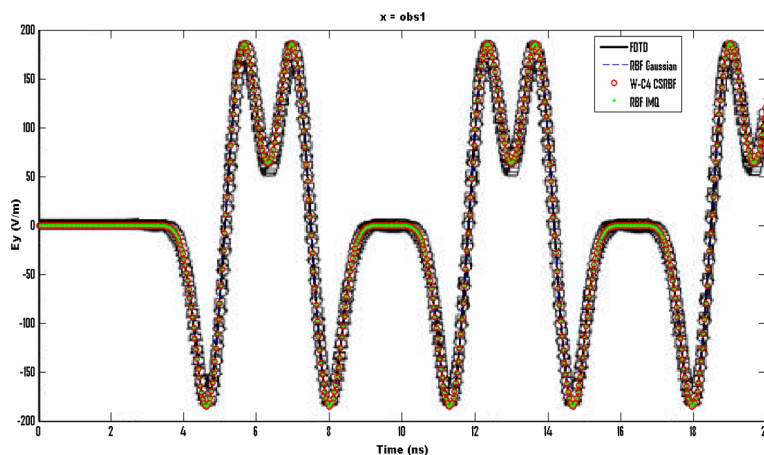


Figure 3. E_y at observation point *obs1* using PEC boundary condition

Figure 4 shows that on one hand, a comparison of the spatial profiles of propagation computed respectively to RBF method at three types of local support with each and on the other hand, the same results of RBF method with the FDTD method at $t=10\text{ns}$, $t=15\text{ns}$ and $t=20\text{ns}$ where identical results were obtained.

In order to show consistency in the computing scheme for long term time arguments as well as for both the RBF Method and the FDTD, the spatial distribution of E_y are plotted in Figure 5 at $t= 150 \text{ ns}$, where the comparison showed identical results. The results obtained by RBF-FDTD was compared with the results shown in Figure 6 from Lai et al. (2008) are identical.

Through this comparison, the choice of the type of support and the number of points do not affect completely the results obtained.

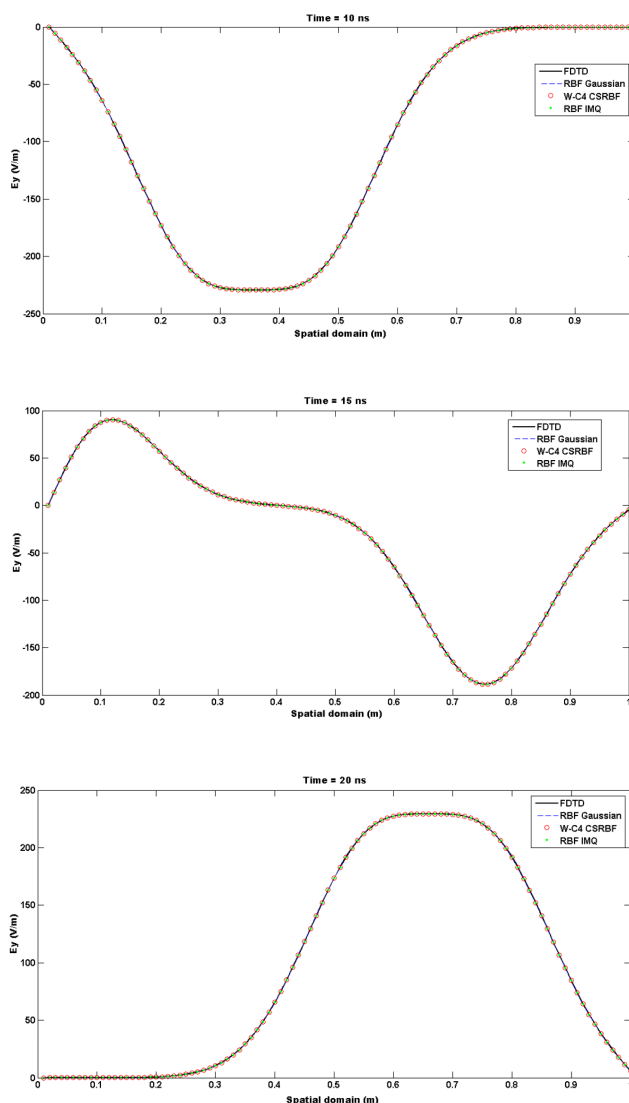


Figure 4. Evolution of E_y spatial profiles for FDTD and RBF method at $t=10 \text{ ns}$ (a), $t=15\text{ns}$ (b) and $t=20 \text{ ns}$ (c), using PEC boundary condition.

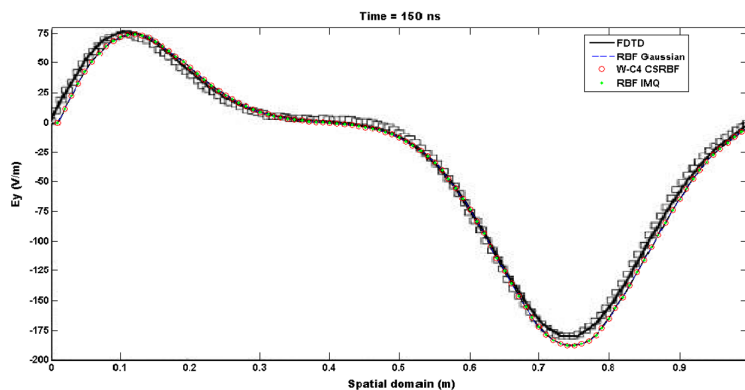


Figure 5. E_y spatial profiles given by RBF- FDTD method at $t= 150$ ns, using PEC boundary condition.

CONCLUSION

In this research, a comparison was performed between the conventional FDTD and RBF methods with radial basis functions. The numerical results showed that the numerical stability of the proposed method is related to the radius of a local support domain and the shape parameters of basis functions. Yet, the construction of the shape function matrix in local RBF method is more complex than that of the global RBF method. Moreover, the use of locally Gaussian and CSRBF basis function is more complex than that of the IMQ; otherwise, the previous basis functions have a problem of stability. In order to eliminate the instability programming process of the above two basis functions, each node in the local support must have its own suitable parameter. It was found that the use of RBF method is very economical in terms of computation time and programming burden.

REFERENCES

- Belytschko, T., Krongauz, Y., Organ, D., Fleming, M., & Krysl, P. (1996). Meshless methods: an overview and recent developments. *Computer Methods in Applied Mechanics and Engineering*, 139(1), 3-47.
- Cingoski, V., Miyamoto, N., & Yamashita, H. (1998). Element-free Galerkin method for electromagnetic field computations. *Magnetics, IEEE Transactions on*, 34(5), 3236-3239..
- Fasshauer, G. E. (2007). *Meshfree approximation methods with MATLAB (Vol. 6)*. World Scientific Co Pte.Ltd.
- Kansa, E. J. (1990). Multiquadrics—A scattered data approximation scheme with applications to computational fluid-dynamics—II solutions to parabolic, hyperbolic and elliptic partial differential equations. *Computers and Mathematics with Applications*, 19(8), 147-161.
- Kaufmann, T., Yu, Y., Engström, C., Chen, Z., & Fumeaux, C. (2012). Recent developments of the meshless radial point interpolation method for time-domain electromagnetics. *International Journal of Numerical Modelling: Electronic Networks, Devices and Fields*, 25(5-6), 468-489.
- Lai, S. J., Wang, B. Z., & Duan, Y. (2008). Meshless radial basis function method for transient electromagnetic computations. *Magnetics, IEEE Transactions on*, 44(10), 2288-2295.

- Lima, N. Z., Fonseca, A. R., & Mesquita, R. C. (2012). Application of local point interpolation method to electromagnetic problems with material discontinuities using a new visibility criterion. *IEEE Transactions on Magnetics*, 48(2), 615.
- Liu, G. R., & Gu, Y. T. (1999) *A point Interpolation Method*. In the proceeding of 4th Asia-pacific Conference on Computational Mechanics. pp. 1009- 1014.
- Liu, G. R., & Gu, Y. T. (2005). An Introduction to Meshfree Methods and their Programming. *Springer*; Dordrecht, The Netherlands.
- Shaterian, Z., Kaufmann, T., Fumeaux, C. (2012). *Impact of different Node Distributions on Meshless Radial Point Interpolation Method in Time-Domain Electromagnetic Simulations*. Proceeding of APMC, Taiwan.
- Viana, S. A., Rodger, D., & Lai, H. C. (2006). Application of the local radial point interpolation method to solve eddy-current problems. *IEEE transactions on magnetics*, 42(4), 591-594.
- Wang, J. G., & Liu, G. R. (2002). A point interpolation meshless method based on radial basis functions. *International Journal for Numerical Methods in Engineering*, 54(11), 1623-1648.
- Wendland, H. (1995). Piecewise polynomial, positive definite and compactly supported radial functions of minimal degree. *Advances in computational Mathematics*, 4(1), 389-396.